ISSN 1674-1056
http://cpb.iphy.ac.cn
http://iopscience.iop.org/cpb
中国物理 B
Chinese Physics
中国物理 Chinese Physics B

Power of all-fiber amplifier increasing from 1030 W to 2280 W through suppressing mode instability by increasing the seed power

Xue-Xue Luo(罗雪雪), Ru-Mao Tao(陶汝茂), Chen Shi(史尘), Han-Wei Zhang(张汉伟), Xiao-Lin Wang(王小林), Pu Zhou(周朴), Xiao-Jun Xu(许晓军)

Citation: Chin. Phys. B . 2019, 28(2): 024208. **doi:** 10.1088/1674-1056/28/2/024208
Journal homepage: http://cpb.iphy.ac.cn; http://iopscience.iop.org/cpb

What follows is a list of articles you may be interested in

Experimental and numerical investigation of mid-infrared laser in Pr^{3+}-doped chalcogenide fiber

Hua Chen(陈华), Ke-Lun Xia(夏克伦), Zi-Jun Liu(刘自军), Xun-Si Wang(王训四), Xiang-Hua Zhang(章向华), Yin-Sheng Xu(许银生), Shi-Xun Dai(戴世勋)

Chin. Phys. B . 2019, 28(2): 024209. **doi:** 10.1088/1674-1056/28/2/024209

Mode-locked fiber laser with $MoSe_2$ saturable absorber based on evanescent field

Ren-Li Zhang(张仁栗), Jun Wang(王俊), Xiao-Yan Zhang(张晓艳), Jin-Tian Lin(林锦添), Xia Li(李夏), Pei-Wen Kuan(关珮雯), Yan Zhou(周延), Mei-Song Liao(廖梅松), Wei-Qing Gao(高伟清)

Chin. Phys. B . 2019, 28(1): 014207. **doi:** 10.1088/1674-1056/28/1/014207

Carboxyl graphene oxide solution saturable absorber for femtosecond mode-locked erbium-doped fiber laser

Rui-dong Lv(吕瑞东), Lu Li(李璐), Yong-gang Wang(王勇刚), Zhen-dong Chen(陈振东), Si-cong Liu(刘思聪), Xi Wang(王茜), Jiang Wang(王江), Yong-fang Li(李永放)

Chin. Phys. B . 2018, 27(11): 114214. **doi:** 10.1088/1674-1056/27/11/114214

Femtosecond Tm-Ho co-doped fiber laser using a bulk-structured Bi_2Se_3 topological insulator

Jinho Lee(李珍昊), Ju Han Lee(李周翰)

Chin. Phys. B . 2018, 27(9): 094219. **doi:** 10.1088/1674-1056/27/9/094219

Sb_2Te_3 mode-locked ultrafast fiber laser at 1.93 μm

Jintao Wang(王金涛), Jinde Yin(尹金德), Tingchao He(贺廷超), Peiguang Yan(闫培光)

Chin. Phys. B . 2018, 27(8): 084214. **doi:** 10.1088/1674-1056/27/8/084214

Power of all-fiber amplifier increasing from 1030 W to 2280 W through suppressing mode instability by increasing the seed power*

Xue-Xue Luo(罗雪雪)[1], Ru-Mao Tao(陶汝茂)[1,2,3,†], Chen Shi(史尘)[1,2,3], Han-Wei Zhang(张汉伟)[1,2,3], Xiao-Lin Wang(王小林)[1,2,3,‡], Pu Zhou(周朴)[1,2,3], and Xiao-Jun Xu(许晓军)[1,2,3]

[1] *College of Advanced Interdisciplinary Studies, National University of Defense Technology, Changsha* 410073, *China*
[2] *Hunan Provincial Key Laboratory of High Energy Laser Technology, National University of Defense Technology, Changsha* 410073, *China*
[3] *Hunan Provincial Collaborative Innovation Center of High Power Fiber Laser, Changsha* 410073, *China*

(Received 10 September 2018; revised manuscript received 25 October 2018; published online 10 January 2019)

In this work, we investigate suppressing mode instability in detail by varying the seed power in a large mode area all-fiber amplifier with a fiber core diameter of 25 μm. The transverse mode instability (TMI) thresholds are systematically measured for different seed power. Our experimental results reveal that increasing the seed power has a positive influence on enhancing the output power before the TMI effect appears, and finally the TMI threshold is approximately doubled from 1030 W to 2280 W when the seed power is increased from 27 W to 875 W. Almost 84.7% slope efficiency is reached with different seed power before the TMI threshold power. During our operation, we also find that in this type of LMA fiber the beam quality of the amplifier is degraded gradually instead of a sudden change as the pump power increases.

Keywords: mode instabilities, seed power, coupling efficient, beam quality degradation

PACS: 42.55.Wd, 42.55.Xi, 42.65.Es **DOI:** 10.1088/1674-1056/28/2/024208

1. Introduction

In recent years, one of the most outstanding limitations in the evolution of the power scaling of ytterbium doped fiber laser with near diffraction limited beam quality is mode instability.[1–3] Since the first report of this phenomenon,[4] many researchers from different groups have devoted their efforts to the investigation of its underlying physical mechanisms[5–10] and mitigation methods.[11–16] According to the thermal origin of the mode instability, there are more than three techniques that can be used for mitigating the mode instability. The first effective way is to enhance the losses of high-order modes by utilizing new-type fibers,[17,18] optimizing Yb-ion concentration,[19] or coiling active fibers with a relatively small diameter.[20] The second approach is to reduce the thermal load in the active fiber, including optimizing the wavelength of the seed laser and pump sources thus to weaken the influence of quantum defect or photo-darkening effect,[21–23] or employing counter-pump and bi-directional pump configuration.[24] The third method is to remove the long period grating in the active fiber through dynamic mode excitation of the seed laser,[25] timely modulation of the seed power and pump sources with a frequency close to that of the TMI typical peaks.[26,27]

It has experimentally been reported that the mode instability can be suppressed by increasing the seed power in a small range,[28] which has been confirmed by theoretical work.[29,30] Moreover, the non-linear relation of the extracted signal power at the TMI threshold with seed power has been found in Ref. [31], which means that at a low seed power the extracted power increases sharply and then decreases as the seed power increases. However, the previous experimental study was carried out in microstructure fibers with spatial configuration and the power was somewhat low. So far, no detailed study in step-index double cladding large mode area (LMA) fiber with all-fiber configuration has been presented.

In this paper, our objective is to enhance the mode instability threshold power by changing the seed laser power experimentally, which can be achieved in a high power LMA all-fiber amplifier with a core diameter of 25 μm by employing a counter-pump configuration. In our experiment, the TMI threshold increases from 1030 W to 2280 W while the seed power increases from 27 W to 875 W. Unlike the microstructure fibers, the M^2 of the amplifier using the LMA fiber goes through a gradual change from 1.7 to 2.1 when mode instability happens. Consequently, we present experimental results to verify these TMI suppression theories relating to the seed power.

2. Experimental setup

A counter-pump scheme was used in the fiber amplifier, as shown in Fig. 1. The master oscillator was a linear cavity, including a pair of fiber Bragg gratings (FBGs) and ytterbium-doped fiber (YDF). The high-reflector (HR) FBG with a refractive rate of 99% and an output-coupler (OC) FBG of 10%

*Project supported by the National Natural Science Foundation of China (Grant Nos. 61735007 and 61505260).
†Corresponding author. E-mail: taorumao@sohu.com
‡Corresponding author. E-mail: chinawxllin@163.com
© 2019 Chinese Physical Society and IOP Publishing Ltd

were centered at a wavelength of ∼ 1080 nm. The ∼ 1080-nm wavelength range was chosen to avoid amplifying the stimulated emission effect in the oscillator. The gain medium utilized in the laser oscillator was double cladding YDF with a core diameter of 20 μm and an inner cladding diameter of 400 μm. The YDF is coiled from a diameter of 15 cm to 20 cm. Nine fiber-pigtailed 976-nm lase diodes (LDs) were used to pump the laser oscillator, which enable the system to achieve a maximal output power of 875 W. The cladding light strippers (CLSs) were performed in a piece of 20/400 μm germanium-doped fiber (GDF), which can help to strip the unabsorbed pumping light propagated in and high-order signal light leaked out from the inner cladding, but which does not influence the output laser in the fiber core. The GDF used in the experimental configuration has 1 dB/km cladding attenuation at 1095 nm and thus will not take on any spatial nor spectral filtering effects. Both the CLSs and GDFs can only be used to obtain better laser quality and propagate nearly non-loss laser. Before the amplifier, the 20/400 μm GDF was related to another piece of 25/400 μm GDF to lessen the harmful effect of the core diameter mismatching problem. The 13-m active fiber utilized in the power amplifier had a core diameter of 25 μm and the cladding absorption coefficient of the active fiber is 1.28 dB/m at 976 nm. Then, the output seed light of the oscillator was launched into the power amplifier before passing through the signal port of a $(6+1)\times 1$ signal/pump combiner. The signal input port and output port fibers of the combiner have the same core diameter of 25 μm, and the inner cladding diameters are 400 μm and 250 μm respectively. The pump power was provided by LDs with a center wavelength of 976 nm, which were combined by six power combiners, and then injected into six pump ports of the combiner with 220/242 μm fibers. The maximum output power of each LD in the amplifier was 110 W. CLSs were performed after the counter-pump combiner in a similar way to that in the laser oscillator. One end cap (QBH) was spliced to deliver the output power and avoid any end-face reflection, which has an input port with 25/400 μm fiber. All of these components were fixed on a water-cooled heat sink with the exception of the end cap.

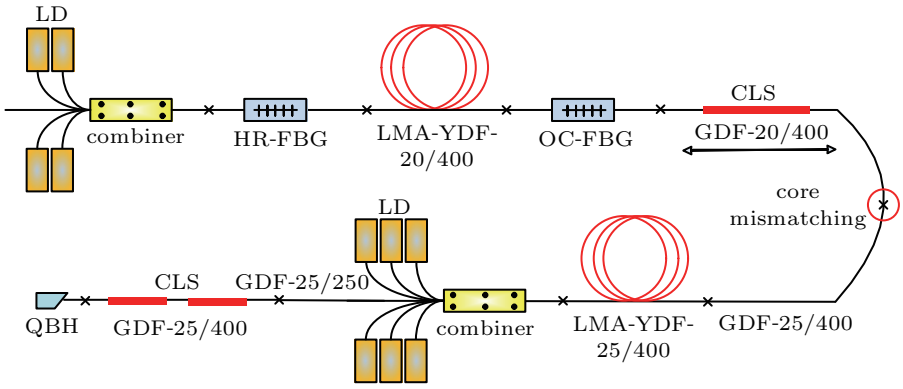


Fig. 1. Experimental schematic diagram.

3. Results and analysis

3.1. Characteristics of master oscillator

To fully understand the influence of the seed power on the mode instability in fiber amplifier, we first measure the output power and the beam quality of the master oscillator. Figure 2(a) shows the output power of the seed laser versus pump power. When the pump power is tuned to 970 W, the output power reaches 875 W. Figure 2(b) shows the far-field beam spot image with different seed power and we only measure up to 703 W. In Fig. 2(c), the measured M^2 of seed laser shows stability and equilibrium in the rectangular coordinate system. Our results show that as the seed power increases, the beam quality degrades slightly. For the dots of 27-W and 512-W seed powers, the corresponding values of M^2 are 1.15 and 1.20, which shows no apparent distinction. And even when the power reaches 703 W, the beam quality is still below 1.3.

3.2. Threshold of mode instability with different seed powers

We measure the output power of the amplifier with different fixed seed powers. The results in Fig. 3 show that in each seed power, when the pump power is increased to a certain value, the amplifier efficiency will decrease. When further adding the pump power, the output power will also decrease, which means that the slope efficiency of the amplifier turns negative and there is a roll over point in the amplifier in each seed power. The active fiber is coiled with a small diameter in the experiment, after the active fiber CLSs are used to strip the residual pump light and high-order modes (HOM) light in the amplifier. In this case, when the pump power reaches the TMI threshold, the higher modes generated in the amplifier will be stripped, and therefore the output power will decrease.[32] Hence, we can define the output power of the roll over point as the threshold of mode instability. From the results we can see

that the threshold power increases with seed power increasing. For example, when the seed power is 27 W, the threshold is only 1030 W. But when increasing the seed power to 124 W, the threshold is more than 1500 W, and at last the threshold almost reaches 2300 W when the seed power is 875 W. The increase of the seed power has a positive influence on mitigating TMI since the enhancement of seed laser power can lessen the population inversion, thus strengthening the gain saturation effect. With stronger gain saturation, which can affect the forming of modal coupling field between the fundamental mode and high-order modes, the TMI threshold power can be higher.[30] In each seed power condition, the corresponding slope efficiency before the roll over point is about 84.7%.

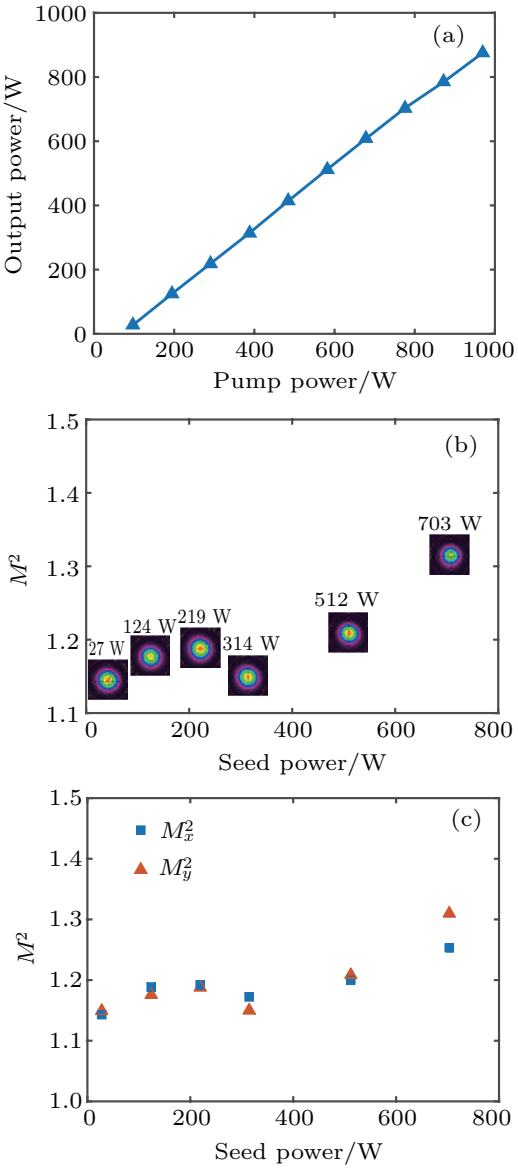


Fig. 2. Characteristics of the master oscillator: (a) output power versus pump power of oscillator, (b) measured beam spot image, and (c) measured values of M^2 versus seed power of seed laser.

To validate the mode instability effect and its threshold, we position a detector to record the temporal change of the output power by using the same method as referred in Ref. [20]. In the experiment, an InGaAs photodetector (150 MHz, 700 nm–1800 nm) is used to detect the scattering light from the power meter. Taking 875-W seed power for example, time traces at 1570-W and 2280-W output powers are shown in Fig. 4(a). The output beam stays stable and shows no fluctuation when output power is 1570 W. While output power reaches 2280 W, the beam profile becomes unstable with the time trace fluctuating. We can obtain the frequency distributions of the beam fluctuation in Fig. 4(b) by the Fourier analysis of the time traces to calculate the corresponding Fourier spectra. From the figure it is obvious that the frequency domain becomes a little bit chaotic around 2.5 kHz when mode instability appears.

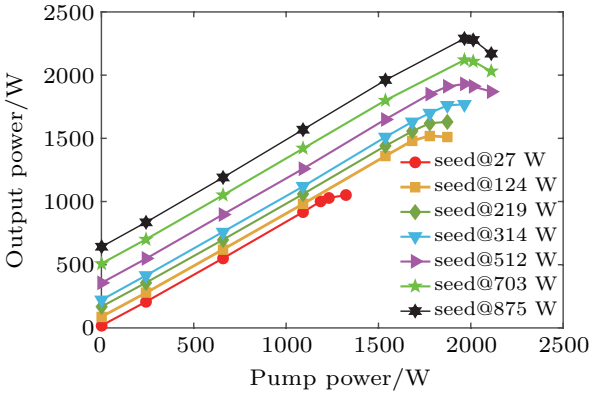


Fig. 3. Plots of output power versus pump power at different seed power.

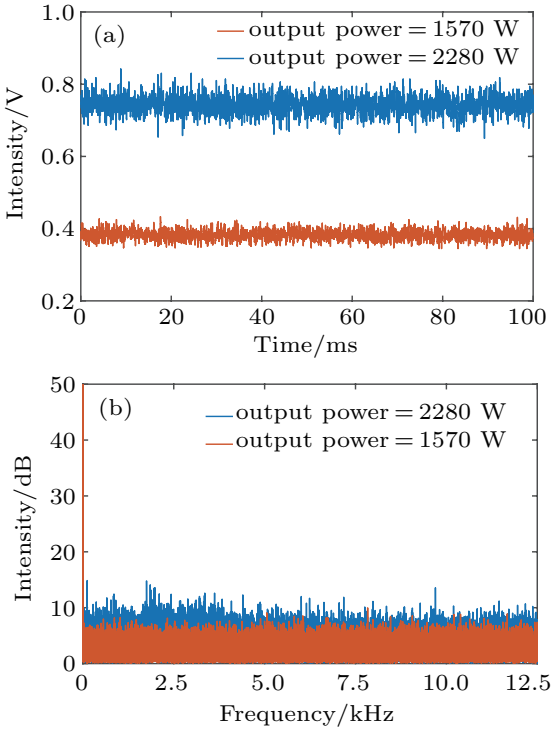


Fig. 4. Experimental results for 875-W seed power showing (a) time traces and (b) frequency traces, at output power of 1570 W and 2280 W.

By using the definition in Ref. [33], we can calculate the TMI threshold based on the time domain results of the photodetector, thereby approving our definition of the threshold

power by using the roll over point. The σ representing the undulating degree in time domain can be expressed as

$$\sigma = \left[\frac{\int_0^{15\ \mathrm{kHz}} P(\nu)\mathrm{d}\nu}{\int_{15\ \mathrm{kHz}}^{30\ \mathrm{kHz}} P(\nu)\mathrm{d}\nu} - 1\right] \times 100\%, \quad (1)$$

where $P(\nu)$ is the power density at frequency ν. In the calculation process, σ remains low below the TMI threshold, which means that $P(\nu)$ stays stable in a frequency range of -30 kHz. The onset of TMI will arouse some frequency components in a range of 0 kHz–15 kHz, which leads to a sharp increase of σ, and we adopt the definition that threshold power is reached once σ increases up to 10%. In this way, like the 875-W seed power, the TMI threshold power is calculated to be about 2280 W when σ equals 10%. In Fig. 5, we present the calculated σ values of various pump power for 875-W seed power. Meanwhile, the measured TMI threshold power for the roll over point at 875-W seed power in Fig. 3 is 2290 W. Compared with the calculated one, the power differs by only 10 W. And we also compare the calculated results with measured results at 512-W and 703-W seed powers, which are 1920 W–1930 W and 2130 W–2120 W respectively. Thus, it can be proven that our definition of the roll over point to measure the TMI threshold power is effective and accurate.

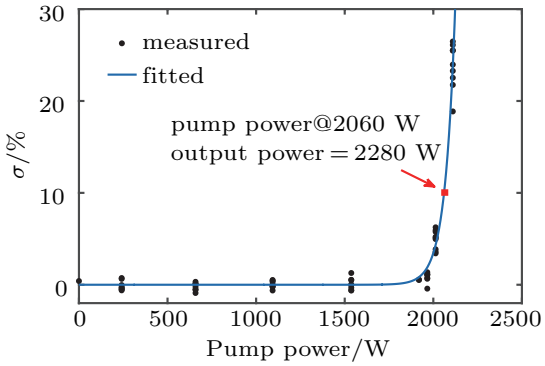


Fig. 5. Plot of calculated σ versus pump power.

We also measure the beam quality of output laser at different pump power for 875-W seed power. An apparent degradation process before TMI happened is shown in Fig. 6(a). From the figure, it can be seen that with the output power increasing, the beam quality deteriorates gradually instead of a sudden change of the appearance of TMI.[34] When the threshold power 2280 W is reached, the value of M^2 drops from 1.7, when no pump light passes through the amplifier to 2.1. From the beam spot image in Fig. 6(a) it can be seen that when the output power reaches nearly to 2000 W, the fundamental mode signal light starts to fluctuate and becomes unstable, which is influenced by the stimulation of high-order modes light. This is because of the multiple-mode supportive character in the 25-μm core fiber, some high-order-mode laser can be stimulated and amplified in the fiber even when the output power is relatively low. With a certain proportion of high-order modal signal light in the output laser, M^2 results go through a gradual degradation process, which differs from the scenario of our experiment in which the fibers are other types of fibers. Considering that the reflection mirror is directly exposed to high power laser light for the M^2 testing time, the laser caused relatively high temperature and thermal effect can harm the test results. Then, we measure the spectrum of the output signal laser at the threshold power so that we can check whether the stimulated Raman scattering (SRS) appears. The result in Fig. 6(b) shows that there is no SRS except for the signal laser with a ratio of 30-dB peak intensity at 2280-W threshold power.

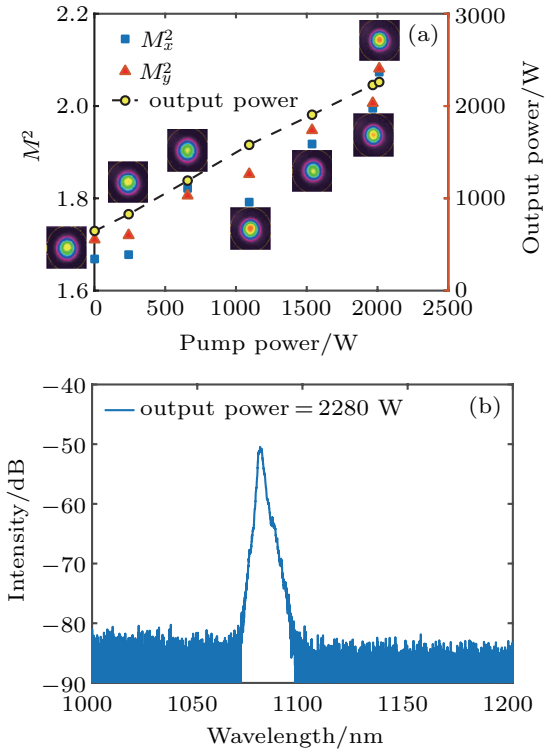


Fig. 6. Experimental results for 875-W seed power, showing (a) M^2 and output power versus pump power, and (b) spectrum of the 2280-W signal laser.

To further study the influence of seed laser power on suppressing the TMI effect, we calculate the threshold using Eq. (1) and extract signal power in each seed power[35] as shown in Fig. 7. For a low seed power, the TMI threshold power and extracted signal power grow nonlinearly and sharply. For instance, the threshold power is 1030 W for 27-W seed power, while it ups to 1380 W for 124-W seed power and then only increases to 1550 W for 219-W seed power. This means that when seed power is lower than 200 W, its positive influence on suppressing TMI is very significant. While the seed power is above 200 W, the TMI threshold still increase but the extracted signal power seems only to gain slightly, and it finally reaches a stable value of about 1410 W for above 500-W seed power. By utilizing the increasing seed power method we successfully obtain a factor of 100% improvement output power from 1030 W to 2280 W.

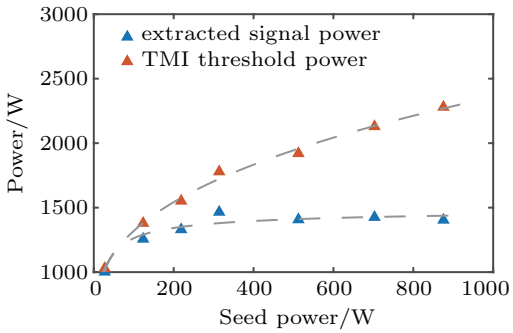


Fig. 7. Plots of calculated TMI threshold power and extracted signal power versus seed power.

4. Conclusions

In this work, we demonstrate a TMI suppression method in a high power large mode area all-fiber amplifier system by increasing seed power and finally acquire a 2280-W high-power output. Our results show that for 27-W seed power the TMI threshold power is 1030 W and the extracted signal power is 1003 W, and it then increases to 1380 W and 1256 W for 124-W seed power. Finally, the threshold power ups to 2280 W for 875-W seed power. However, the extracted signal power seems to obtain a stable result around 1410 W for above 500-W seed power. In other words, increasing the seed power has a limited influence on suppressing the TMI effect, but it is still a promising approach to enhance the fiber amplifier power scale. When we further increase the seed power, the SRS may appear, which needs further study.

Acknowledgment

The authors would like to thank Mr. Xiaoyong Xu, Mr. Kun Zhang, Mr. Lin Chen and Miss Siliu Liu for their assistance in the whole experiment.

References

[1] Wirth C, Schmidt O, Tsybin I, Schreiber T, Eberhardt R, Limpert J, Tünnermann A, Ludewigt K, Gowin M, Have E and Jung M 2011 *Opt. Lett.* **36** 3118
[2] Eidam T, Wirth C, Jauregui C, Stutzki F, Jansen F, Otto H, Schmidt O, Schreiber T, Limpert J, and Tünnermann A 2011 *Opt. Express* **19** 13218
[3] Jauregui C, Limpert J and Tunnermann A 2013 *Nat. Photon.* **7** 861
[4] Eidam T, Hanf S, Seise E, Andersen Thomas V, Gabler T, Wirth C, Schreiber T, Limpert J and Tünnermann A 2010 *Opt. Lett.* **35** 94
[5] Ward B, Robin C and Dajani I 2012 *Opt. Express* **20** 11407
[6] Smith A V and Smith J J 2011 *Opt. Express* **19** 10180
[7] Jauregui C, Eidam T, Limpert J and Tünnermann A 2011 *Opt. Express* **19** 3258
[8] Jauregui C, Eidam T, Otto H, Stutzki F, Jansen F, Limpert J and Tünnermann A 2012 *Opt. Express* **20** 12912
[9] Smith A V and Smith J J 2013 *Opt. Express* **21** 2606
[10] Otto H, Modsching N, Jauregui C, Limpert J, Tünnermann A 2015 *Opt. Express* **23** 15265
[11] Kent E M 2009 *Opt. Express* **17** 17855
[12] Haarlammert N, Sattler B, Liem A, Strecker M, Nold J, Schreiber T, Eberhardt R, Tünnermann A, Ludewigt K and Jung M 2015 *European Conference on Lasers and Electro-Optics — European Quantum Electronics Conference*, June 21–25, 2015, Munich, CJ_10_3
[13] Li T L, Zha C W, SuncY H, Ma Y, Ke W W and Peng W J 2018 *Laser Physics* **28** 105101
[14] Jauregui C, Otto H J, Stutzki F, Jansen F, Limpert J and Tünnermann A 2014 *SPIE* **8961** 896128
[15] Smith A V and Smith J J 2013 *Opt. Express* **21** 15168
[16] Hejaz K, Norouzey A, Poozesh R, Heidariazar A, Roohforouz A, Nasirabad R R, Jafari N T, Golshan A H, Babazadeh A and Lafouti M 2014 *Laser Phys.* **24** 025102
[17] Laurila M, Saby J, Alkeskjold T T, Scolari L, Cocquelin B, Salin F, Broeng J and Lægsgaard J 2011 *Opt. Express* **19** 10824
[18] Murao T, Saitoh K and Koshiba M 2011 *Opt. Express* **19** 1713
[19] Tino E, Steffen H, Jansen F, Stutzki F and Rothhardt J 2011 *Opt. Express* **19** 8656
[20] Tao R M, Ma P F, Wang X L, Zhou P and Liu Z J 2015 *Photon. Res.* **3** 86
[21] Tao R M, Ma P F, Wang X L, Zhou P and Liu Z J 2015 *J. Opt.* **17** 45504
[22] Jauregui C, Otto H, Stutzki F, Jansen F, Limpert J and Tünnermann A 2013 *Opt. Express* **21** 19375
[23] Tao R M, Ma P F, Wang X L, Zhou P and Liu Z J 2015 *IEEE J. Quantum Electron.* **51** 1
[24] Shi C, Su R T, Zhang H W, Yang B L, Wang X L, Zhou P, Xu X J and Lu Q S 2017 *IEEE Photon. J.* **9** 1502910
[25] Otto H, Jauregui C, Stutzki F, Jansen F, Limpert J and Tünnerman A 2013 *Opt. Express* **21** 17285
[26] Stihler C, Jauregui C, Limpert J and Tünnermann A 2017 *European Conference on Lasers and Electro-Optics — European Quantum Electronics Conference*, June 25–29, 2017, Munich, CJ_6_4
[27] Stihler C, Jauregui C, Otto H, Limpert J and Tünnermann A 2017 *SPIE* **10083** 100830P
[28] Laurila M, Jørgensen M M, Hansen K R, Alkeskjold T T, Broeng J and Lægsgaard J 2012 *Opt. Express* **20** 5742
[29] Naderi S, Dajani I, Madden T and Robin C 2013 *Opt. Express* **21** 16111
[30] Tao R M, Wang X L, Zhou P and Xu X J 2017 *J. Opt.* **19** 065202
[31] Jauregui C, Otto H, Stutzki F, Limpert J and Tünnermann A 2015 *Opt. Express* **23** 20203
[32] Wang X L, Tao R M, Xiao H, Zhou P, Zhang C D and Xu X J 2013 *Advance Solid-State Laser*, October 27–November 1, 2013, Paris, JTh2A.44
[33] Tao R M, Ma P F, Wang X L, Zhou P and Liu Z J 2016 *J. Opt.* **18** 065501
[34] Wirth C, SchreiberT, Rekas M, Tsybin I, Peschel T, Eberhardt R and Tünnermann A 2010 *SPIE* **7580** 75801
[35] Otto H J, Jauregui C, Stutzki F, Jansen F, Limpert J and Tünnermann A 2013 *Advanced Solid-State Lasers*, October 27–November 1, 2013, Paris, ATu3A.02